

# X-ray obscuration in local Universe AGN

Matteo Guainazzi

*European Space Astronomy Center, Apartado 50727, E-28080 Madrid, Spain*

**Abstract.** I review the constraints that X-ray observations impose on the physical properties and the geometrical distribution of cold absorbing gas in nearby obscured Active Galactic Nuclei (AGN), as well as their implications for AGN structure models.

## INTRODUCTION

It has been known since the dawn of X-ray spectroscopy that the high-energy emission of type 2 Active Galactic Nuclei (AGN) is obscured by large column densities of cold and neutral gas [1, 2]. This discovery nicely matches the predictions of the standard Seyfert unification scenario [3, 4], which ascribes the “type 1” versus “type 2” dichotomy to our line-of-sight orientation with respect to an azimuthally symmetric dust molecular “torus”, preventing the direct view of the central engine and of the Broad Line Regions (BLRs) in the latter.

After almost twenty years of Seyfert 2 galaxies X-ray observations: which constraints can we derive on the physical properties and on the geometrical distribution of the X-ray obscuring matter? Which relations exist between the X-ray absorbing gas and material responsible for obscuration or reddening at other wavelengths? Which are the implications of these results for the AGN structure models? I will address these question in this contribution.

A bit of terminology before starting: X-ray obscured AGN can be classified into “Compton-thin” or “-thick” depending on the column density,  $N_H$ , covering the nuclear emission. In objects belonging to the latter class  $N_H \gtrsim \sigma_t^{-1} \sim 1.6 \times 10^{24} \text{ cm}^{-2}$ . The direct nuclear emission of Compton-thick Seyfert 2s is totally suppressed in the 0.1–10 keV energy band, where most of sensitive X-ray observations have been performed so far. Even in this band, however, Compton-thick Seyfert 2 galaxies are not totally silent: the flat continuum measured in most of them, together with the large Equivalent Width ( $EW > 1 \text{ keV}$ ) iron  $K_\alpha$  fluorescent line, indicates a dominant contribution by Compton-reflection off optically-thick matter, most likely illuminated by the intrinsic AGN continuum through an unobscured optical path. Traditionally, X-ray spectra of Compton-thick object are referred to as “reflection-dominated” (and those of Compton-thin objects as “transmission-dominated”). Although there are good reasons to believe that this association does not always hold [5, 6] we will maintain it throughout this paper for simplicity. Finally, some of the experimental evidence presented in this paper refer to optically-thick X-ray reprocessing rather than to X-ray absorption. Whenever pertinent, I will make explicit the physical reasons, allowing us to extend to the latter the conclusions derived for the former.

# PROPERTIES OF OPTICALLY-THICK GAS IN THE AGN ENVIRONMENT FROM X-RAY OBSERVATIONS

## Column density distribution

Several independent studies of optically-selected Seyfert 2s samples suggest that the distribution of column densities in the local Universe is flat in logarithmic scale across the whole range between  $10^{22}$  and  $10^{25} \text{ cm}^{-2}$  [7, 8]<sup>1</sup>. They are confirmed by the results of a complete, volume-limited sample of AGN observed by XMM-Newton [10]. On the basis of a O[III] selected sub-sample of the RXTE All-Sky Survey [11], Heckman et al. [12] estimate that the fraction of Compton-thick AGN over the total number of Seyfert 2 galaxies in the local Universe is  $36 \pm 14\%$ . The existence of “elusive” AGN [13], where optical signatures of nuclear activity are missing, implies that the above estimate could be actually only a lower limit to the true number.

Such a large fraction of highly-obsured AGN should be present at cosmological distances as well. The  $N_H$  distribution can be constrained by comparing the spectrum of the Cosmic X-ray Background (CXB) with models producing it through the superposition of unresolved AGN [14, 15]. Indeed, the intrinsic column density distribution in large X-ray surveys is consistent with being flat [16]. Nonetheless, recent results from a survey of more than 127 AGN detected by INTEGRAL IBIS/ISGRI above 20 keV [17] unveil a fraction of Compton-thick AGN ( $\sim 10\%$ ) significantly lower than predicted by CXB models. However, as the same authors point out in their paper, this result has to be taken with caution, because the X-ray emission of “very Compton-thick objects” ( $N_H \gtrsim 10^{25-26} \text{ cm}^{-2}$ ) is expected to be significantly suppressed by Compton scattering even in the INTEGRAL energy band.

## Location

The measurement of the soft photoelectric spectral cut-off allows us to measure the column density integrated along the whole line of sight to the AGN. Hence, X-rays can provide constraints on the distribution and location of optically thick gas only from direct high-resolution imaging observations, and from variability studies.

In the Circinus Galaxy [18] images in the iron  $K_{\alpha}$  fluorescent emission line band, likely to be dominated by optically-thick reprocessing of the nuclear continuum, are unresolved at the *Chandra* spatial resolution ( $\sim 0.3''$ ). This constrains the size of the line-emitting region to be  $\lesssim 8$  pc. Interestingly enough, in NGC 1068 the hard X-ray emission, including the iron line region, is seen extending  $\sim 2$  kpc [19], with a tentative detection of iron  $K_{\alpha}$  fluorescent line extension up to  $\sim 5.5$  kpc. This evidence is in contradiction with the compact size of the torus as derived from the interferometric measurements in this object [20]. In more distant Compton-thick AGN the constraints drawn from direct iron imaging are looser. However, indirect constraints on the compact-

---

<sup>1</sup> On the other hand, radio-loud samples seem to be missing highly obscured AGN [9].

ness of the reflector can be drawn from the lack of photoelectric “shadows” on AGN-photoionized gas extending on scales as large as 0.1-1 kpc [21].

Evidence for compact cold gas in the nuclear environment comes also from the detection of rapid variability of the X-ray absorber. A breakthrough discovery in this field was the detection of one order of magnitude variation of the absorber column density between two RXTE observations of NGC 4388 taken 4 hours apart [22]. If explained by occultation of a gas cloud ( $N_H = 3 \times 10^{22}$ ) in Keplerian motion around the supermassive black hole, the inferred cloud location ( $\sim 10^3$  Schwarzschild radii) is typical of the BLR scale rather than of the standard “torus” envisaged by the Seyfert unification scenario. The same conclusions were drawn by Puccetti et al. (2004) [23] from a similar episode detected in NGC 4151. An even more extreme episode of variability has been recently detected during an intense monitoring campaign of the Compton-thick Seyfert 2 galaxy NGC 1365. This AGN has been shown to exhibit changes from a “reflection-” to a “transmission-dominated” status in less than two days (See Elvis et al., this volume). All these pieces of observational evidence suggest that, at least in some objects, the gas responsible for the X-ray obscuration is close to the central engine. Risaliti et al. (2002) speculate that it could be associated with accretion disk dust-free outflows, in the framework of the model of AGN structure proposed by Elvis (2000).

On the other hand, observational evidence exists, which associate the Compton-thin X-ray absorber with matter located on scales much larger than the nuclear environment. First of all, good quality spectra of several nearby AGN exhibit simultaneous signatures of obscuration and/or reprocessing by Compton-thick matter and of absorption by Compton-thin matter (NGC 424, [26]; NGC 5506, [27]; NGC 7582, Piconcelli et al., in preparation). The spectral transitions observed in “changing-look” Seyfert 2 galaxies [5, 6] can be explained as a change in the optical path along which we are looking at the AGN emission, due to extreme variability of the AGN intrinsic output. In either state, the optical path intercepts a compact Compton-thick absorber, or a Compton-thin absorber external to the former, respectively (see as well Guainazzi et al. 2004 [28] for a possible case of a Compton-thin absorber covering the spectrum produced by Compton-thick reprocessing). Finally, a study of the X-ray absorption properties of a Seyfert 2 sample selected according to nuclear dust morphology on  $\gtrsim 100$  pc scale [29] led Guainazzi et al. (2005) [8] to conclude that Compton-thin Seyfert 2s are preferentially located in “dusty” nuclear environments, whereas Compton-thick Seyfert 2 galaxies are equally distributed between nuclear “dusty” and “not-dusty” host galaxies. These pieces of evidence suggest that X-ray Compton-thick and -thin absorbers are physically decoupled. The former is probably very compact (typical scales  $\lesssim 1$  pc), the latter is likely to be associated to host galaxy dust lanes on scales  $\gtrsim 100$  pc. The possible role of host galaxy dust in shaping the AGN classification had already been suggested by Maiolino & Rieke (1995) and Malkan et al (1998) [29, 30].

## Geometry and covering fraction

It is difficult to get direct X-ray observational constraints on the geometry of the X-ray absorber and/or reflector. One of the most promising methods is the detection of

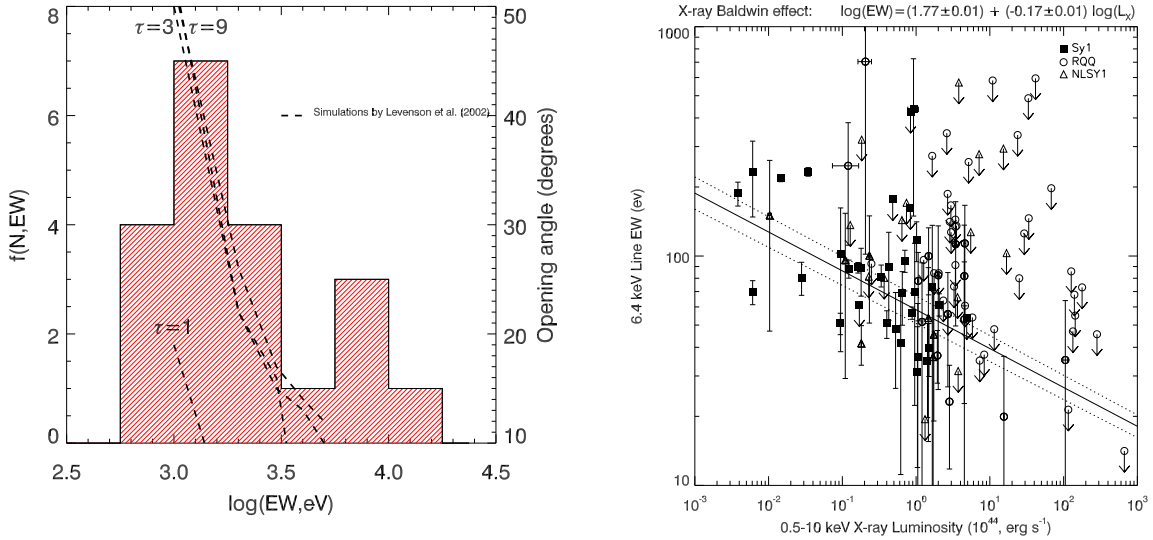


**FIGURE 1.** *Left panel:* the hatched histogram represents the iron  $K_{\alpha}$  fluorescent line EW distribution in an optically selected sample of Compton-thick Seyfert 2 galaxies observed by XMM-Newton [8]. The dashed lines represent the opening angle of optically thick gas in a torus-like structure required to produce a given EW for different values of the Thompson optical depths [35, 36, 37]. *Right panel:* anti-correlation between the iron  $K_{\alpha}$  fluorescent line EW and the X-ray luminosity (the “X-ray Baldwin effect” or “Iwasawa effect”) in a large sample of unobscured AGN observed by XMM-Newton (Bianchi et al., in preparation).

the iron  $K_{\alpha}$  fluorescent line Compton Shoulder in objects, where the column density of the gas covering the nuclear emission is known. The relative intensity of the Compton Shoulder with respect to the  $K_{\alpha}$  is a function of the reflector column density and of the line-of-sight inclination [31, 32]. The measurement of the Compton Shoulder in the *Chandra* HETG spectrum of the Circinus Galaxy [33] led to the conclusion that the column density of the absorber and of the reflector are the same. If one associate the former (latter) with the closer (farther) side of the same gaseous system, this must have a toroidal symmetry as the “torus” envisaged by the Seyfert unification scenarios.

Regardless of the detailed geometry, the covering factor of the reflector must be large to account for the relative intensity of the Compton-reflection component in reflection-dominated spectra (see, *e.g.*, the discussion in Risaliti et al. (2005) [34]), as well as for the iron  $K_{\alpha}$  fluorescent line EWs measured in Compton-thick objects. In the *left panel* of Fig. 1 we compare the distribution of the EWs in an optically-defined sample of nearby ( $z \leq 0.035$ ) Compton-thick Seyfert 2 galaxies observed by XMM-Newton [8] with the predictions of Monte-Carlo simulations [35, 36, 37]. Even for extreme Thompson optical depths, EWs larger than 1 keV require opening angles lower than  $30^{\circ}$ , corresponding to a solid angle covering  $\gtrsim 80\%$  of the sky as seen by the central engine.

The covering fraction of the circumnuclear obscuring/absorbing gas is probably not a cosmological invariant. There are at least two independent pieces of experimental evidence supporting this conclusion. The existence of the so-called “Iwasawa effect” (an anti-correlation between the EW of the iron  $K_{\alpha}$  fluorescent line and the X-ray

luminosity<sup>2</sup>, originally discovered by Iwasawa & Taniguchi (1993) [39]) seems now to be definitively demonstrated (Bianchi et al., in preparation; see the *right panel* of Fig. 1), after some controversy on possible sample selection effects [40, 41]. Moreover, the analysis of different X-ray surveys suggests that the fraction of AGN obscured by a column density larger than  $10^{22} \text{ cm}^{-2}$  decreases with the 2–10 keV luminosity. Both the above pieces of evidence can be simultaneously explained by the “receding torus” model, whereby the covering fraction of the obscuring/reflecting gas decreases with luminosity due to a flattening of the dust distribution when the radiation pressure is stronger [42]. Alternatively, low-luminosity AGN could more likely contain dusty walls supported by radiation pressure from a circumnuclear starburst [43]. The possible role of a luminosity-dependent ionization parameter was originally discussed by Mushotzky & Ferland (1984) [44], and, more recently, by Nayakshin (2000a, 2000b) [45, 46] in the context of a disc origin for the narrow iron  $K_{\alpha}$  fluorescent iron line.

## Metallicity

The metallicity of the reflector can be in principle determined through measurements of the iron  $K_{\alpha}$  photoionization edge at  $\gtrsim 7$  keV in reflection-dominated spectra. However, this measurement is very challenging, due to the drop in the effective area of CCD detectors above 6 keV. So far, this measurement has been possible only on NGC 1068 [47] and the Circinus Galaxy [48]. In both cases, an iron overabundance by a factor 1.5–2.5 is required. This is in good agreement with independent pieces of evidence, which suggest very high-metallicity for the gas in the nuclear environment [49, 50].

## IMPLICATIONS FOR AGN STRUCTURE MODELS

One of the immediate consequences of the standard Seyfert unification scenarios is that type 1 AGN should be unaffected by obscuration from the gas, which prevents the direct view of the BLRs. This prediction can now be tested on a sound statistical basis, thanks to large samples of AGN discovered in *Chandra* and XMM-Newton surveys. This basic prediction is verified. There are still a number of exceptions: the fraction of X-ray obscured type 1 AGN ranges between 10% and 30% depending on the sample [10, 51, 52, 53]. The column densities associated to these obscured type 1 AGN are generally lower than  $10^{22} \text{ cm}^{-2}$ . They can be easily accounted for by matter (dust lanes, molecular clouds, etc.) in the host galaxy. As such, this evidence does not pose any substantial problem for the viability of the unified scenarios.

More challenging has been the discovery of a fair number of Seyfert 2 galaxies, which do not show any X-ray obscuration [54, 55]. Wolter et al. (2005) [56] even report the discovery of three type 2 QSO objects (X-ray luminosity  $\sim 10^{44} \text{ erg s}^{-1}$ ),

---

<sup>2</sup> In this context, we discuss only of the Iwasawa effect applied to the narrow component of the iron  $K_{\alpha}$  fluorescent line. A discussion on a possible similar effect affecting the relativistically broadened component of the same emission line can be found in Guainazzi et al. 2006 [38]

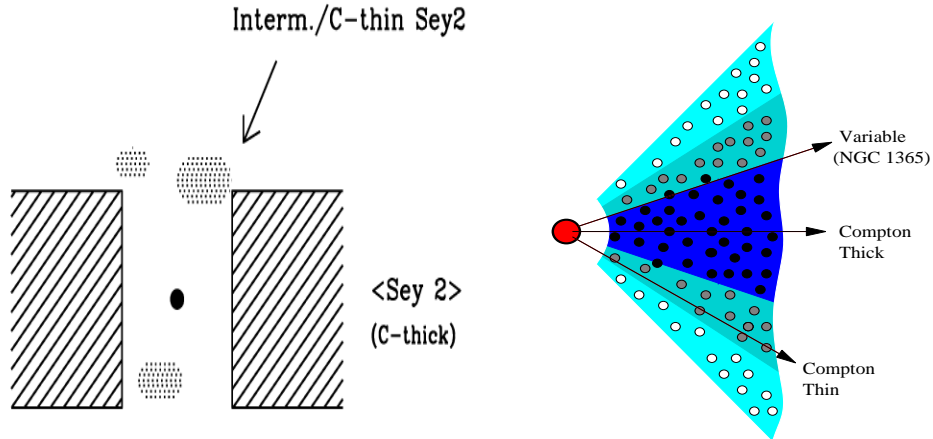


**FIGURE 2.** *Left panel:* Scheme of the unification model for obscured AGN after Matt (2000) [60]; hatched rectangles: Compton-thick gas; dotted ellipses: large scale Compton-thin material. The figure is not in scale. *Right panel:* scheme of the X-ray obscuring system for NGC 1356, after Risaliti et al. (2005) [34]

whose X-ray spectrum is fully unobscured. Variability is a possible explanation, as the optical observations on which the AGN classification is based are almost never simultaneous with the X-ray observations. However, this explanation can be ruled out in the only case, for which simultaneous observations in the two bands were purposely performed (Mkn 993, [57]). Alternatively, the mismatch between the optical and the X-ray classification might point to the existence of “pure” type 2 objects, where the BLRs are absent. An interesting explanation has been proposed by Nicastro (2000) and Nicastro et al. (2003) [58, 59], who suggested that BLRs are formed by accretion disk instabilities occurring in proximity of the radius where the disk changes from a gas pressure to a radiation pressure dominated regime. In this context, the existence of BLRs requires a minimum critical accretion rate: below such a threshold, the transition radius becomes smaller than the innermost stable orbit, and BLRs cannot form.

Fig. 2 shows two simplified schemes of the X-ray absorber geometry, as proposed by Matt (2000) and Risaliti et al. (2005), respectively [34, 60]. Both schemes envisage a physical decoupling between Compton-thick and Compton-thin obscuration. In the former scheme, Compton-thick obscuration is primarily due to compact optically-thick matter in the nuclear environment; the most straightforward identification for this absorbing system (but not the only one!) is the “torus” envisaged by the Seyfert unification scenarios. Compton-thin obscuration should be instead due to matter located on much larger scales, possibly associated to the host galaxy. A viable dynamical model in this framework has been recently presented by Lamastra et al. (2006) [61]. In the latter scheme, the X-ray absorbing system is due to a disk outflow, whose column density decrease with azimuth (see Matt et al. (2000) [62] for tentative evidence of a dependence of the X-ray column density on the disk-torus system inclination angle). Notwithstanding possible further complications due to the contribution of region of intense star formation to the X-ray obscuration [43], or to the interplay between optically-thick matter

and highly-ionized outflows [63, 64], each of the above scenarios explains some of the evidence presented in this paper, but none explains all of them simultaneously. It is therefore likely that both of them are telling us part of the truth. The true geometry and distribution of the obscuring matter is probably rather complex. Different components may correspond to different spatial scales. Some of these components are affected by dynamical or magneto-hydrodynamical instabilities, which imprint their signature on the variability of the X-ray obscuration detected in some objects [24]. On the other hand, any physically motivated models for the “dusty torus” require an extended structure, where the ratio between the outer and the inner radius is  $\simeq 10-100$  [65, 66, 67].

## ACKNOWLEDGMENTS

I warmly thank Dr. S. Bianchi for providing me with the right panel of Fig. 1 prior to publication. This paper reflects intense discussions with a number of collaborators: S. Bianchi, A.C. Fabian, K. Iwasawa, G. Matt, G.C. Perola, E. Piconcelli, P. Rodriguez-Pascual. This paper is partly based on observations obtained with XMM-Newton, an ESA science mission with instruments and contributions directly funded by ESA Member States and the USA (NASA).

## REFERENCES

1. Turner T.J., Pounds K., *MNRAS* **240**, 833–880 (1989)
2. Awaki H., et al., *PASJ* **43**, 195–212 (1991)
3. Antonucci R.R.J., Miller J.S., *ApJ* **297**, 621–632 (1985)
4. Antonucci R., *ARA&A* **31**, 473–521 (1993)
5. Matt G., et al., *MNRAS* **342**, 422–426 (2003)
6. Guainazzi M., et al., *MNRAS* **356**, 295–308 (2005)
7. Risaliti G., et al., *ApJ* **522**, 157–164 (1999)
8. Guainazzi M., et al., *A&A* **444**, 119–132 (2005)
9. Grandi P., et al., *ApJ* **642**, 113–125 (2006)
10. Cappi M., et al., *A&A* **446**, 459–470 (2006)
11. Revnivtsev M., et al., *A&A* **418**, 927–936 (2004)
12. Heckman T.M., et al., *ApJ* **634**, 161–168 (2005)
13. Maiolino R., et al., *MNRAS* **344**, L59–L64 (2003)
14. Setti G., Woltjer L., *A&A* **224**, L21–L23 (1989)
15. Comastri A., et al., *A&A* **296**, 1–12 (1995)
16. La Franca F., et al., *ApJ* **635**, 864–879 (2005)
17. Sazonov S., et al., *astroph/0608418* (2006)
18. Sambruna R., et al., *ApJ* **546**, L13–L17 (2001)
19. Young A.J., et al., *ApJ* **556**, 6–23 (2001)
20. Jaffe W., et al., *Nat* **429**, 47–49 (2004)
21. Bianchi S., et al., *A&A* **448** 499–511 (2006)
22. Elvis M., et al., *ApJ* **615**, L25–L28 (2004)
23. Puccetti S., et al., *NuPhS* **132**, 225–228 (1004)
24. Risaliti G., et al., *ApJ* **571**, 234–246 (2002)
25. Elvis M., *ApJ* **545**, 63–76 (2000)
26. Matt G., et al., *A&A* **399**, 519–523 (2003)
27. Bianchi S., et al., *A&A* **402**, 141–149 (2003)
28. Guainazzi M., et al., *MNRAS* **355**, 297–306 (2004)

29. Malkan M.A., et al., *ApJS* **117**, 25– (1998)
30. Maiolino R., et al., *ApJ* **446**, 561–573 (1995)
31. Sunyaev R.A. & Churazov E.M., *Ast.Lett.* **22**, 649–663 (1996)
32. Matt G., *MNRAS* **337**, 147–150 (2002)
33. Bianchi S., et al., *MNRAS* **322**, 669–680 (2001)
34. Risaliti G., et al., *ApJ* **523**, L93–L96 (2005)
35. Krolik J.H., et al., *ApJ* **420**, L57–L61 (1994)
36. Levenson N.A., et al., *ApJ* **573**, L81–L84 (2002)
37. Levenson N.A., et al., *ApJ* **618**, 167–177 (2005)
38. Guainazzi M., et al., *astroph/0610151* (2006)
39. Iwasawa K. & Taniguchi Y., *ApJ* **413**, L15–L18 (1993)
40. Page K.L., et al., *MNRAS* **347**, 316–322 (2004)
41. Jiménez-Bailón E., et al., *A&A* **435**, 449–457 (2005)
42. Königl A. & Kartje J.F., *ApJ* **434**, 446–467 (1994)
43. Ohsuga K. & Umemura M., *ApJ* **559**, 157–166 (2001)
44. Mushotzky R. & Ferland G.J., *ApJ* **278**, 558 (1984)
45. Nayakshin S., *ApJ* **534**, 718–722 (2000a)
46. Nayakshin S., *ApJ* **540**, L37–L40 (2000b)
47. Matt G., et al., *A&A* **414**, 155–161 (2004)
48. Molendi S., et al., *MNRAS* **343**, L1–L4 (2003)
49. Groves B.A., et al., *MNRAS* **371**, 1559–1569 (2006)
50. Nagao T., et al., *A&A* **447**, 863–876 (2006)
51. Caccianiga A., et al., *A&A* **416**, 901–915 (2004)
52. Mateos S., et al., *A&A* **433**, 855–873 (2005)
53. Tozzi P., et al., *A&A* **451**, 457–474 (2006)
54. Pappa A., et al., *MNRAS* **326**, 995–1006 (2001)
55. Panessa F. & Bassani L., *A&A* **394**, 435–442 (2002)
56. Wolter A., et al., *A&A* **444**, 165–174 (2005)
57. Corral A., et al., *A&A* **431**, 97–102 (2005)
58. Nicastro F., *ApJ* **530**, L65–L68 (2000)
59. Nicastro F., et al., *ApJ* **589**, L13–L16 (2003)
60. Matt G., *A&A* **355**, L31–L33 (2000)
61. Lamastra A., et al., *A&A* **449**, 551–558 (2006)
62. Matt G., et al., *MNRAS* **318**, 173–179 (2000)
63. Blustin A.J., et al., *A&A* **431**, 111–125 (2005)
64. Kinkhabwala A., et al., *ApJ* **575**, 732–746 (2002)
65. Efstathiou A. & Rowan-Robinson M., *MNRAS* **273**, 649–661 (1995)
66. Granato G.L., et al., *ApJ* **486**, 147– (1997)
67. Nenkova M., et al., *ApJ* **570**, L9–L12 (2002)